# Carrier suppression system to measure phase noise of acoustic resonators with low motional resistance

A. Pokharel,[1] E. Vaillant,[1] J. Imbaud,[1] J.J. Boy,[1] F. X. Esnault,[2] and F. Sthal,[1,a]

[1] *FEMTO-ST Institute, Univ. Bourgogne Franche-Comté, CNRS, ENSMM, Besançon, 25000, France*

[2] *Microwave, Digital & Optic Dept., Centre National d'Etudes Spatiales, Toulouse, 31400, France*

A carrier suppression system is implemented in order to measure the phase noise of acoustic resonators that have a low motional resistance. Special adapters' system using transformers is proposed to improve the loaded quality factor of the resonators. With this developped device and described protocol, the inherent noise of resonators can be obtained without an usual electronical oscillator conditionning that could take part in the results. The loaded quality factor is improved from about 10 to 60 percent of the intrinsic quality factor. As an example, the system is used to study Langatate crystal resonators vibrating at 10 MHz. Langatate crystal can be an alternative to substitute the quartz crystal resonators for frequency and time applications. Its coupling coefficient and the product quality factor-frequency is normally higher than in quartz crystal resonators. For ultrastable resonators, the motional resistance obtained with Langatate crystal is about five times lower than for the quartz crystal, it can reach typically few ohms. These resonators have been characterized in terms of impedance, Q-factors, turnover temperature, amplitude-frequency effect, and phase noise. The short-term stability of these resonators is given in terms of Allan standard deviation. Influence of the driving power is presented.

## I. INTRODUCTION

Carrier suppression techniques to measure phase noise were demonstrated by K. H. Sann[1] in 1968 and then by C. H. Horn[2] in 1969. Several configurations in metrology applications have been proposed by F. Walls.[3] These techniques have been used in the microwave band, along with some modifications and improvements.[4,5] Characterization of quartz crystal resonators with this kind of system started in the beginning of 2000.[6,7] The inherent phase stability of crystal resonators is measured in a passive circuit without the noise usually associated with the active oscillator. Conversion of phase noise into short-term stability has been adjusted in 2013.[8] The interesting part of this measurement method is to give a very low noise floor around −150 dBc/Hz at 1 Hz and −160 dBc/Hz at 10 Hz depending on the driving power of the resonators. In the last decade, the measurements of ultrastable quartz crystal resonators have been performed in order to find explanation on the origin of the $1/f$ flicker noise.[9,10] Comparison of different piezoelectric materials could have a great interest in this quest. This method brings an answer about

the absolute noise that could be reached by the overall oscillator. Until now, the usual studied quartz crystal resonators always had a motional resistance higher than the classical fifty ohms used in all bench components. Then, the loaded quality factor of the resonators observed in the measurement system can easily exhibit fifty to sixty percent of the unloaded quality factor as when it is inserted in the sustaining electronic. It is not the case using Langatate crystal ($La_3Ga_{5.5}Ta_{0.5}O_{14}$) also called LGT.[11] The first 10 MHz ultrastable LGT oscillators whose fractional frequency stability and noise almost similar to quartz oscillators i.e. $10^{-13}$ and -110 dBc/Hz at 1 Hz were published in 2008.[12] First attempt to measure the phase noise of LGT resonators in a passive way i.e. without an oscillator was done in 2010 but with low-level performance resonators.[13,14] In this paper, resonators vibrating at 10 MHz are built with very high quality LGT crystal and have been measured on an advanced phase noise measurement system. Because of an impedance value lower than 10 Ω at the resonance, special adaptation was done using transformers to maximize the loaded Q-factor. The impedance bridges have been simulated using an advance optimization process with a simulator in Pspice. Previously, the resonators were characterized in terms of impedance, turnover temperature, and amplitude-frequency effect. The resulting short-term stability of the resonators measured on their metrological vibrating C-mode at 10 MHz is reported according to the resonator driving current. With this developped device and described protocol, the inherent noise of resonators can be obtained without an usual electronical oscillator conditionning that could take part in the results.

## II. PHASE NOISE MEASUREMENT SYSTEM
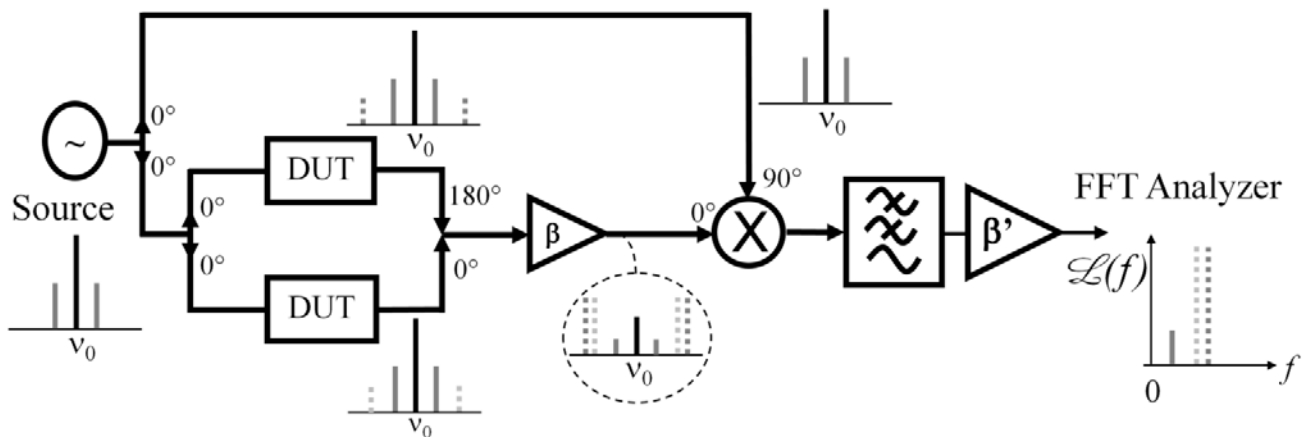
### A. Principle of the bench



FIG. 1. Principle scheme of the measurement system (DUT: Device Under Test).

Figure 1 shows the principle of the measurement system. The low noise excitation source is divided in two parts by a first 0° power splitter. Then, a second 0° power splitter delivers an equal amount of power in both arms. Both arms of the bridge with the Device Under Test (DUT) have similar arrangement of components. Each arm has a phase shifter and an attenuator to adjust the 180° shift to complete the carrier suppression. RF low noise amplifier increases the noise of the DUT while its $1/f$ is maintained at a low level because of the carrier suppression. With a symmetrical mount, the influence of the carrier source is highly reduced. The only remaining fluctuations in output signal would be the noise from the DUT's. Then, a mixer and a low pass filter keeps only the low frequency baseband. Finally, a low noise amplifier increases the output signal that is fed to the FFT analyzer to observe the power spectral density of phase fluctuations. Figure 2 presents the experimental mount.
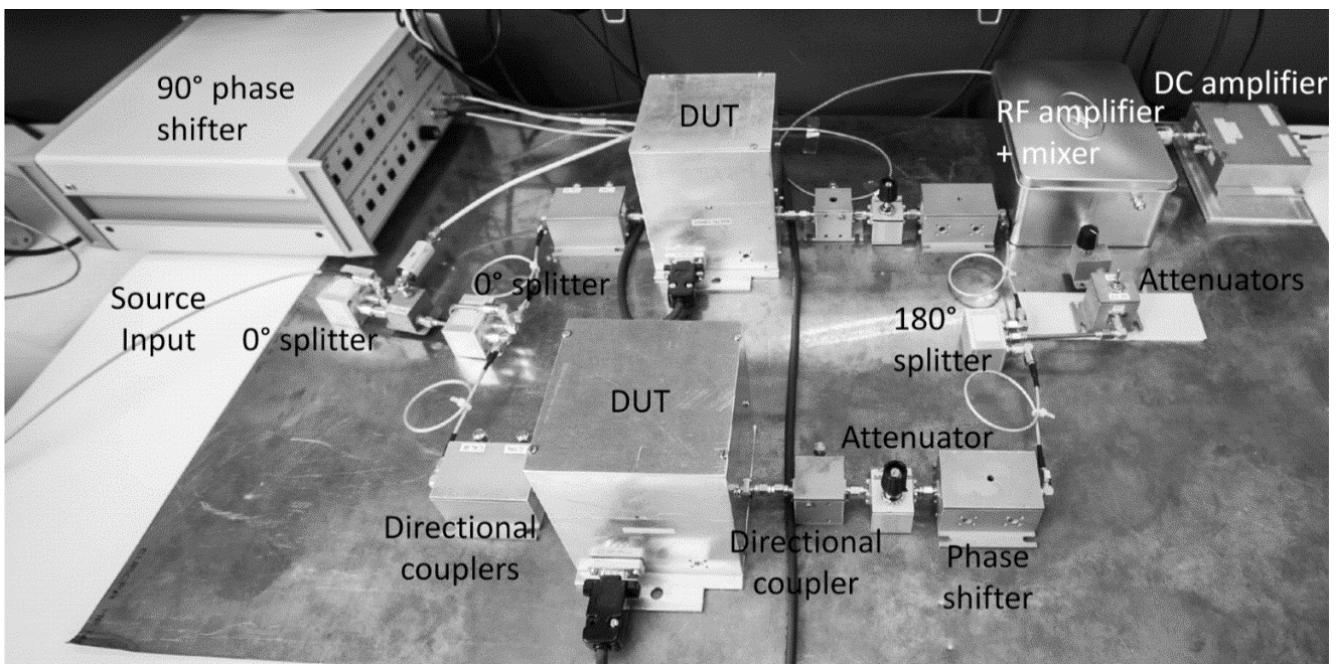


FIG. 2. Phase noise measurement system.

The DUT boxes are temperature controlled in order to get thermal stability when resonators are measured.[15,16] The thermal stability is around 2 μK over a 1s period of time in the heart of the oven. Calibration of the measurement system is obtained by injecting a known sideband on one of the arms of the bridge. The result of the measurement bench is corrected using the calibration factor determined from this sideband.

This bench is essentially used to perform measurements near the carrier, generally until 100 kHz to 1 MHz, farther the DUT noises from the carrier, more it's possible to be hidden by the noise floor of the bench. That is why this bench is

particularly well adapted to measure high (loaded) quality factor resonators which have frequency corner (bandpass filter frequency) relatively low and near the carrier.

## B. Device under test (DUT)

### 1. Classical DUT configuration

All the commercial components of the bench are matched at 50 $\Omega$. Usually, the measured resonators are matched to 50 $\Omega$ using a half $\pi$-bridge build with two external resistor $R_s$ and $R_p$ (Figure 3). The device under tests can possibly be resistors or a pair of crystal resonator to get the noise floor of the system. Resonators are usually associated with a serial capacitor to tune the frequency shift. This configuration is well adapted to resonators that has a motional resistance higher than 50 $\Omega$, usually a case for the quartz crystal resonators.
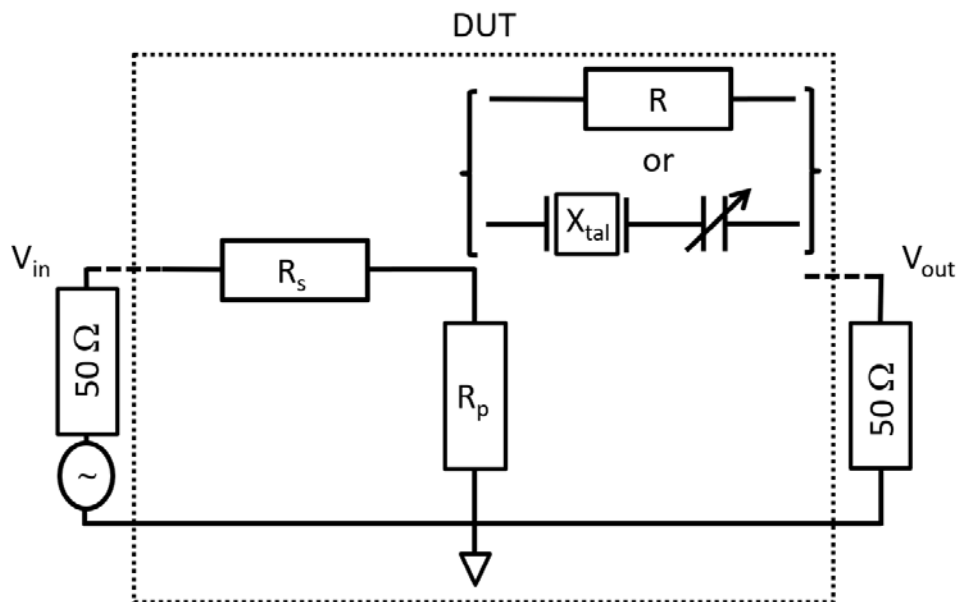
FIG. 3. Usual DUT configuration.

In the usual DUT configuration, Figure 4 presents a transfer function of a 10 MHz quartz crystal resonator SC-cut, with a very high stability. The unloaded quality factor, $Q_0$, is around $1.3 \cdot 10^6$ and its motional resistance is 66 $\Omega$. Using resistor $R_S$ and $R_P$ equal to 30 $\Omega$ and 24 $\Omega$ respectively the loaded quality factor, $Q_L$, is around $0.85 \cdot 10^6$ that represents about 65 % of $Q_0$. In that case the output signal is sufficient to perform the passive noise measurement.

4

Taking into account the relation between the loaded Q factor and the load impedance defined in the International Standard IEC 60444-1[17] as: $Q_L = \frac{\omega_S L_S}{R_S + R_L}$ with $\omega_S$ the serial pulsation, $L_S$ the motional inductance, $R_S$ the serial motional resistance and $R_L$ the load resistance. Table I summarizes the calculated loaded quality factor in the case of a fifty ohms resistive load.

TABLE I. Calculus of the loaded quality factor, $Q_L$, of the resonator loaded with 50 $\Omega$.

| Motional resistance $R_S$ ($\Omega$) | Unloaded Q factor $Q_0$ | Load resistance ($\Omega$) | Calculated motional inductance (H): $L_S = \frac{Q_0 R_S}{\omega_S}$ | Calculated loaded Q factor: $Q_L = \frac{\omega_S L_S}{R_S + R_L}$ |
|---|---|---|---|---|
| 66 | $1.3 \cdot 10^6$ | 50 | 1.365 | 739 358 (56.9% of $Q_0$) |
| 8 | $1 \cdot 10^6$ | 50 | $127.32 \cdot 10^{-3}$ | 137 931 (13.8% of $Q_0$) |

A low value of loaded Q-factor is a problem because the corner frequency will be higher and the signal level lower than at for lower frequency. This means that the measured noise could be below the noise floor of the bench. Moreover, the major inconvenience of the resistive pi network impedance matching is its dissipative effect. Therefore, when the DUT impedance is about tenth of fifty ohms, reaching a high excitation in drive level values can be difficult.
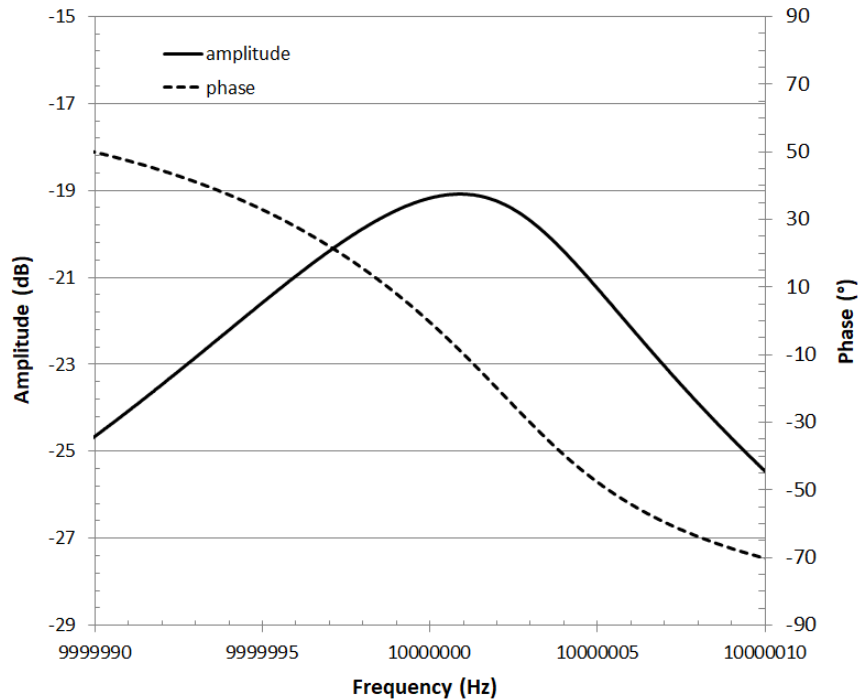


FIG. 4. Transfer function of 10MHz SC-cut Quartz Crystal loaded in the half bridge of figure 3.

## 2. DUT special impedance matching circuit

The motional resistance of 10 MHz LGT resonators is below 10 $\Omega$. Thus, the loaded Q of the final mount cannot be higher than 15 % of the unloaded Q in the case of classical DUT configuration (see Figure 6, with T1-1). Thus, transformer matching is proposed to improve the loaded Q factor of the resonator and maximize the drive level power. Figure 5 shows the special matching circuit.
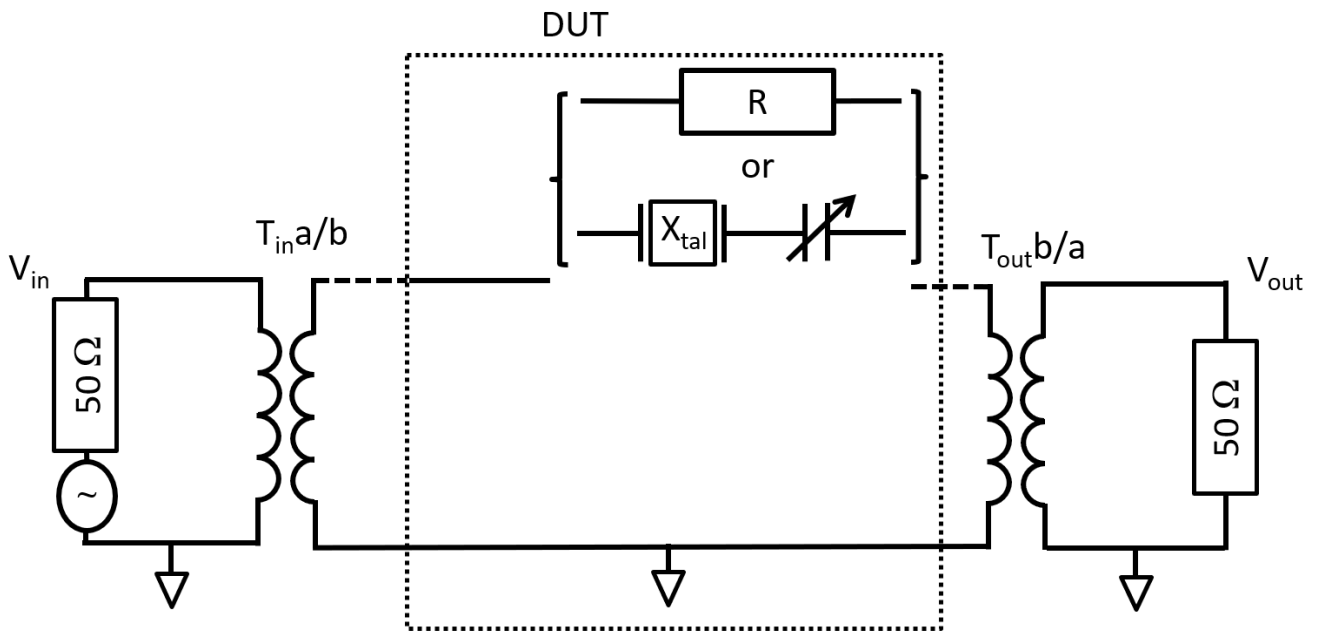


FIG. 5. Low impedance DUT configuration.

Two transformers are inserted before and after the classical DUT configuration. Pspice simulations have been investigated. Figure 6 shows the magnitude and phase of the transfer function of a resonator using the circuit presented in Figure 5. The impedance ratios of the transformers used were 1, 8 and 16. Then, the loaded Q factor of the 10 MHz LGT resonators increased from 10 % to 70 %, respectively. The experimental and simulated values of magnitude and phase are in a good agreement. Small shifts in frequency and phase are induced by the uncertainty in values of the tuning capacitors.
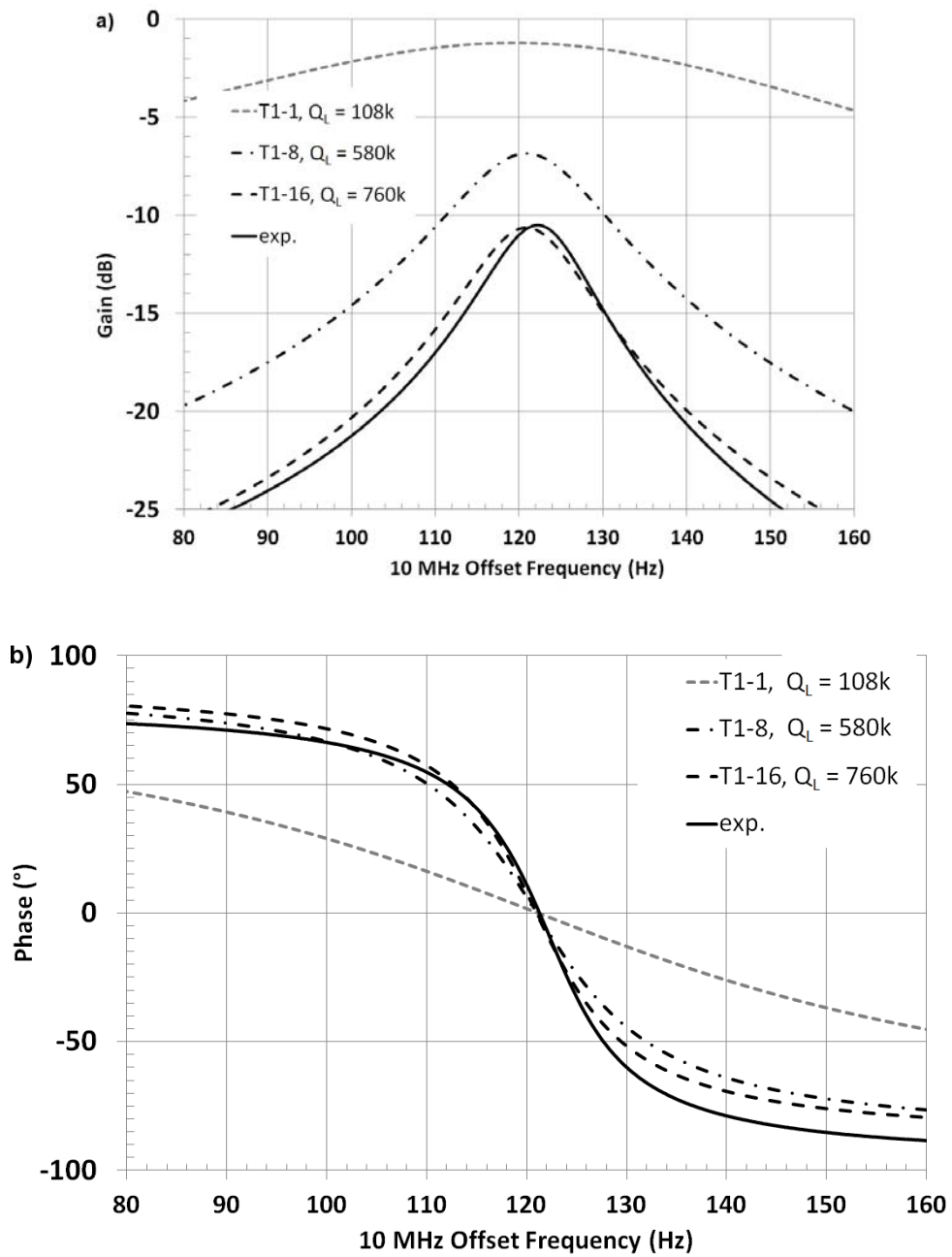
FIG. 6. Amplitude (a) and phase (b) of the transfer functions simulated with some transformer ratios compared to experimental results. The LGT resonator is simulated with 9 Ω resistance.

Figure 7 presents a view of the adaptors. The two transformers are visible on the left side of the picture, the resonator is inserted inside the oven and the tuning capacitor is visible at the right side of the picture.
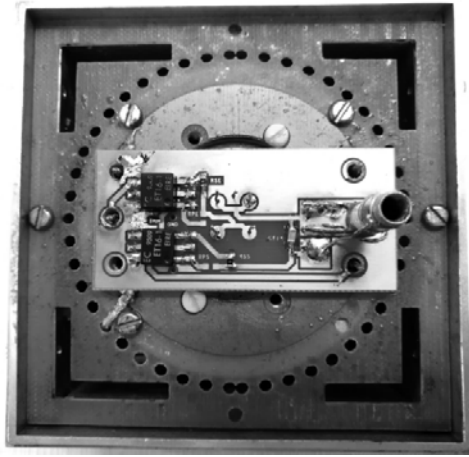
FIG. 7. Transformer adapter with two transformers, resonator inside the oven and the tuning capacitor.

To compare the impedance matching using transformer with a simple pi-bridge resistors, an optimization under Pspice was done for the same input voltage amplitudes that can be seen in Table II (with 9 $\Omega$ resonators and $Q_0$ about $1 \cdot 10^6$). Transformer matching showed a better loaded quality factor about 80 % instead of 55 % obtained using a PI-network. The drive level is also higher due to lower losses.

TABLE II Comparison between transformers and PI resistive impedance matching

|  | PI-network impedance matching | Transformers matching impedance ratio 1:16 |
|---|---|---|
| Gain (dB) | -27 dB | -14dB |
| Loaded Q-factor (% unloaded Q) | 55 % | 80 % |
| Drive level (µW) | 100 µW | 94 µW |

## C. Noise floor of the bench

Figure 8 presents the noise floor of the system using the transformer configuration according the driving power. The working frequency is set at 10.000121 MHz to have the resonance when resonators are inserted.
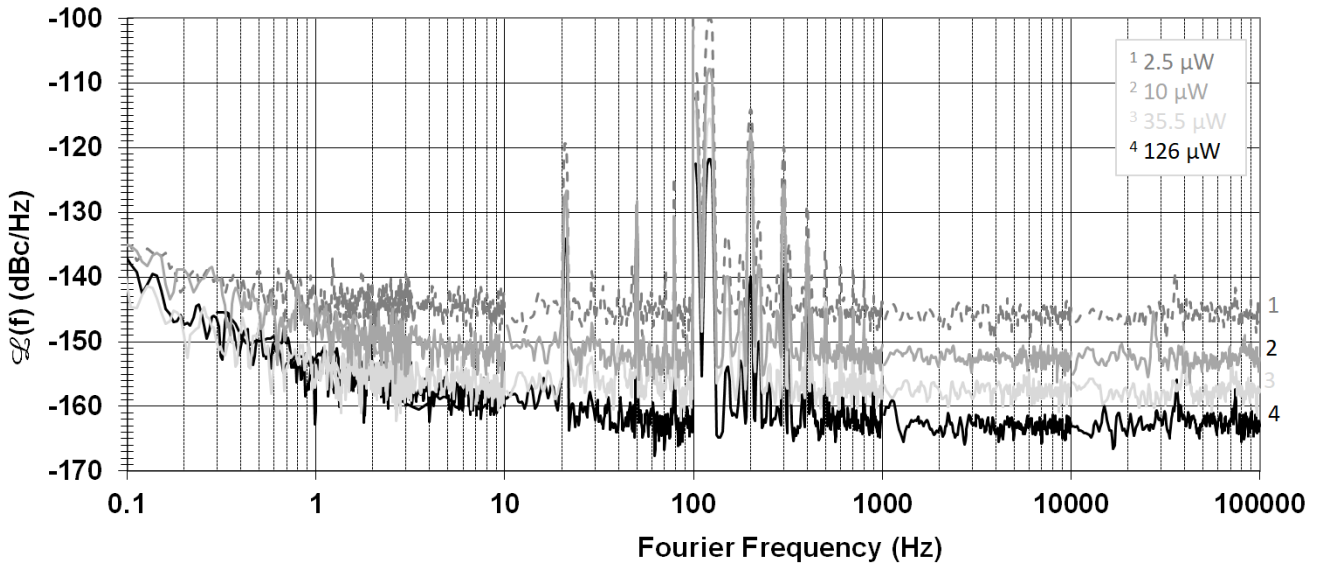
8

FIG. 8. Phase noise of the floor. The source frequency is 10.000121 MHz. The dissipated power is varied from 1.5 to 126 μW.

The noise floor of the system was achieved by inserting an equivalent resistor of 9 Ω replacing the resonator. The excitation power for the resonator was varied for a range of values in micro-watts to see the effect on the phase noise floor introduced by the transformer setup as explained above. There were no unusual effects on the nature of the phase noise floor except for the level of noise floor which is a function of the input power. The noise level is below -145 dBc/Hz at 1 Hz. The thermal noise floor is given by the level of the dissipated power driving the DUTs (around -156 dBc/Hz at 35.5 μW). Spurs on the curves above 10 Hz are because of the mixing between the frequency reference of the synthesizer at 10 MHz and its output signal at 10.000121 MHz. In that case, a spur at 121 Hz can be generated. Other spurs are produced by the power supply of the system (50, 100, 150 ...Hz). Then, mixing between the frequencies at 100 Hz and 121 Hz leads to 21 Hz spur and higher harmonics.

## III. NOISE MEASUREMENT ON LANGATE RESONATORS

The measurement system presented above is used to characterize ultra-stable LGT resonators.

### A. Resonator characteristics

#### 1. Temperature effect

Figure 9 shows the frequency behaviors of the resonators $LGT_{(1)-(3)}$ according to temperature. Turnover temperatures are similar for all resonators and are found around 84 °C. The second order dependencies are given in ppb/°C$^2$ and equal to -67.7, -59.4 and – 72.6 for $LGT_{(1)-(3)}$, respectively. In comparison, the SC-cut type of quartz cut is six times less sensitive[13].
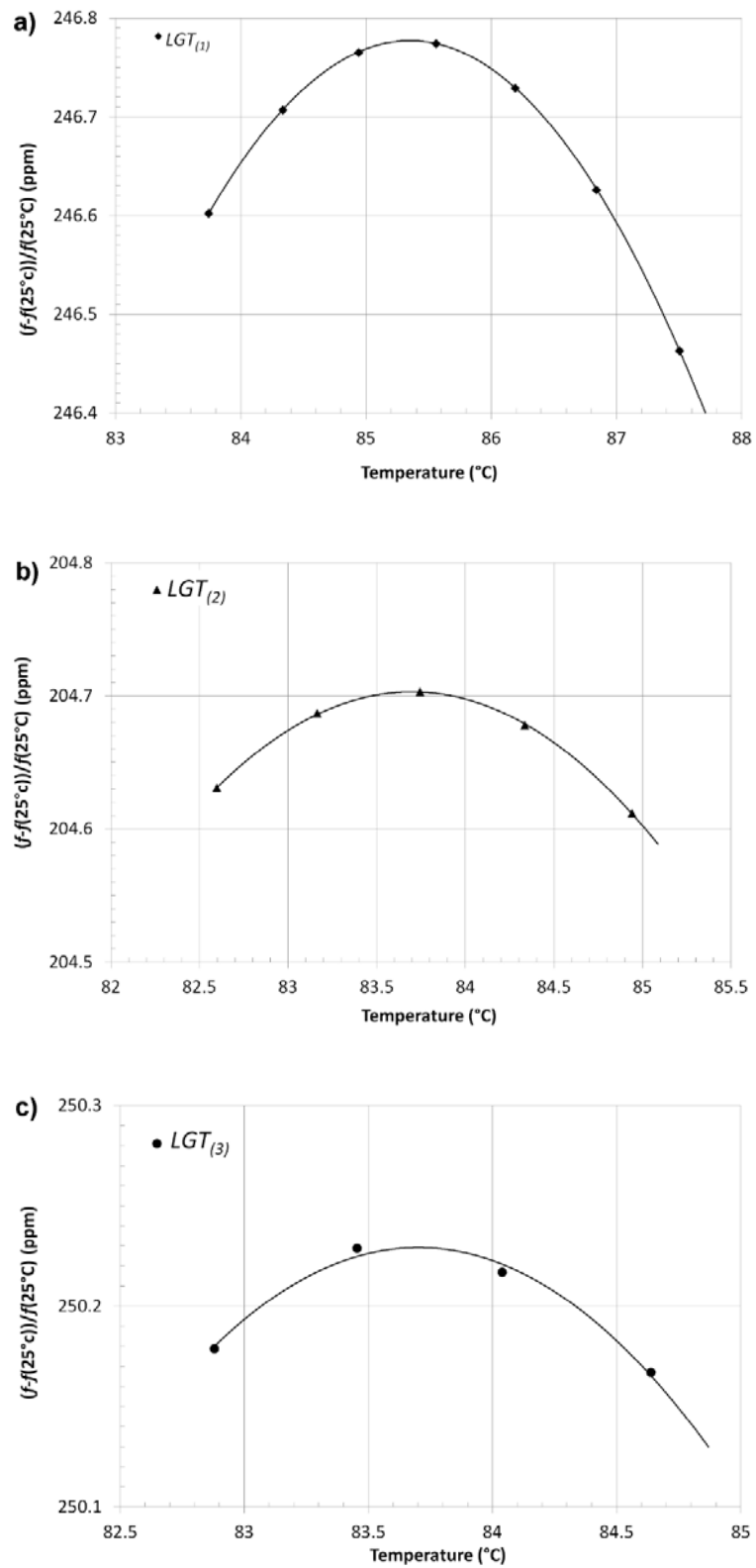
9

FIG. 9. Temperature parabolic curves of LGT resonators. a) resonator $LGT_{(1)}$, b) resonator $LGT_{(2)}$, c) resonator $LGT_{(3)}$.

### *2. Motional parameters*

The used crystal block is synthesized using the Czochralski method[18] and comes from Cristal Innov. The LGT resonators were achieved in Y-1° cut, thus, the turnover temperature is adjusted around 80°C. The applied power to measure the motional parameters is around 60 µW. Figure 10 presents the amplitude and phase of the impedance according the resonant frequencies of three resonators referenced as $LGT_{(1)}$, $LGT_{(2)}$, and $LGT_{(3)}$.
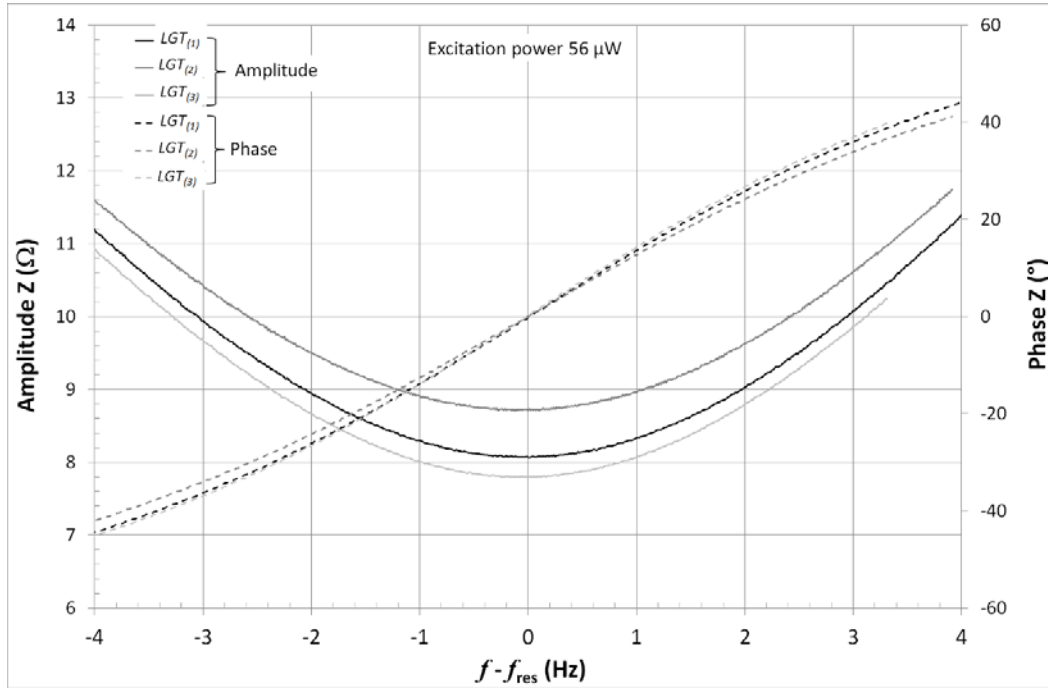


FIG. 10. Amplitude and phase of the resonators $LGT_{(1)-(3)}$, at approximately 60 µW of excitation power.

Table III gives the experimental values of the resonant frequencies at turnover temperatures, the turnover temperatures PI, the motional parameters $R$ and $L$, the static capacitances $C_0$ and the unloaded quality factor $Q$ of the three resonators $LGT_{(1)-(3)}$ respectively. The motional resistance is given by the minimum of the amplitude of impedance. The quality factor is measured from the inverted slope of ±1° phase shift in Figure 10. The motional resistance was found to be around 8 Ω. The unloaded quality factors Q was around $1.1 \cdot 10^6$.

TABLE III. Experimental values of motional parameters and quality factor.

| Res. | $f_{res}$ - 10 MHz (Hz) | $R$ ($\Omega$) | $L$ (mH) | $C_0$ (pF) | $Q$ ($10^6$) |
|------|------|------|------|------|------|
| $LGT_{(1)}$ | 44.8 | 8.1 | 153 | 17.3 | 1.19 |
| $LGT_{(2)}$ | 34.4 | 8.7 | 150 | 17.0 | 1.08 |
| $LGT_{(3)}$ | 29.4 | 7.8 | 158 | 17.2 | 1.27 |

### 3. Driving effect

Figure 11 shows the frequency variation of resonators $LGT_{(1)-(3)}$ according the resonator driving current. The resonator's excitation current was varied from few mA to 10 mA. As observed in Kim (2003)[11], the data set of each resonator is fitted with a quadratic curve to obtain a drive sensitivity coefficient D defined by:

$$\frac{\Delta f}{f} = Di^2$$

The value of D is about -4.2 ppb which is a little bit higher than the values proposed in Kim (2003)[11] but keeps the order of magnitude.
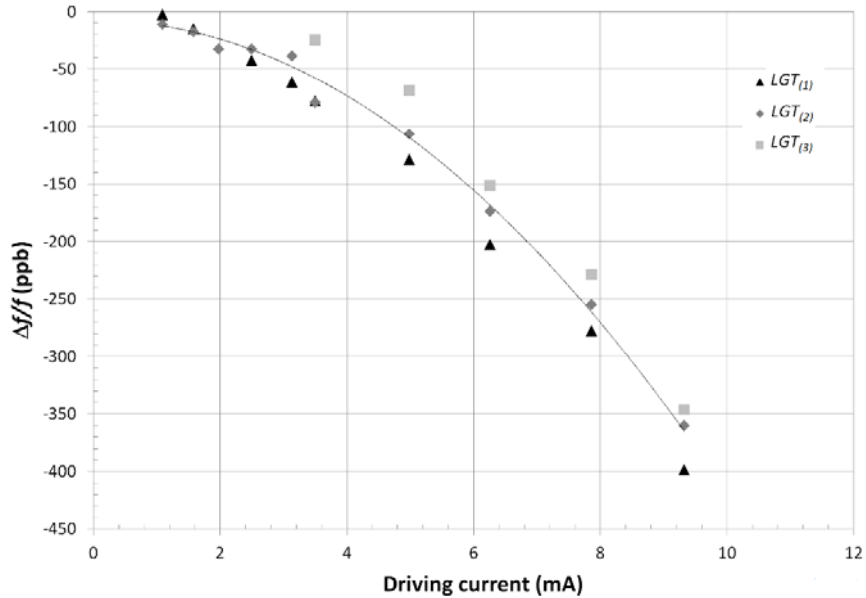


FIG. 11. Frequency variation of the resonators $LGT_{(1)-(3)}$ according to the resonator driving current.

## B. Noise measurements

Figure 12 shows the results in terms of one-sided power spectral density (PSD) of phase fluctuations, $\mathcal{L}(f)$, measured between $LGT_{(1)}$, $LGT_{(2)}$ and $LGT_{(3)}$ resonators. The driving power of the resonator was around 200 µW. Figure 12a presents resonators $LGT_{(1)-(2)}$, Figure 12b $LGT_{(1)-(3)}$, Figure 12c $LGT_{(2)-(3)}$. The measurements were obtained using the T1-16 transformers, hence, the loaded quality factor is optimized as presented in § B.2. The noise of the resonator is visible below 10 Hz Fourier frequency. Above 20 Hz, the behavior is due to the noise floor of the measurement system.
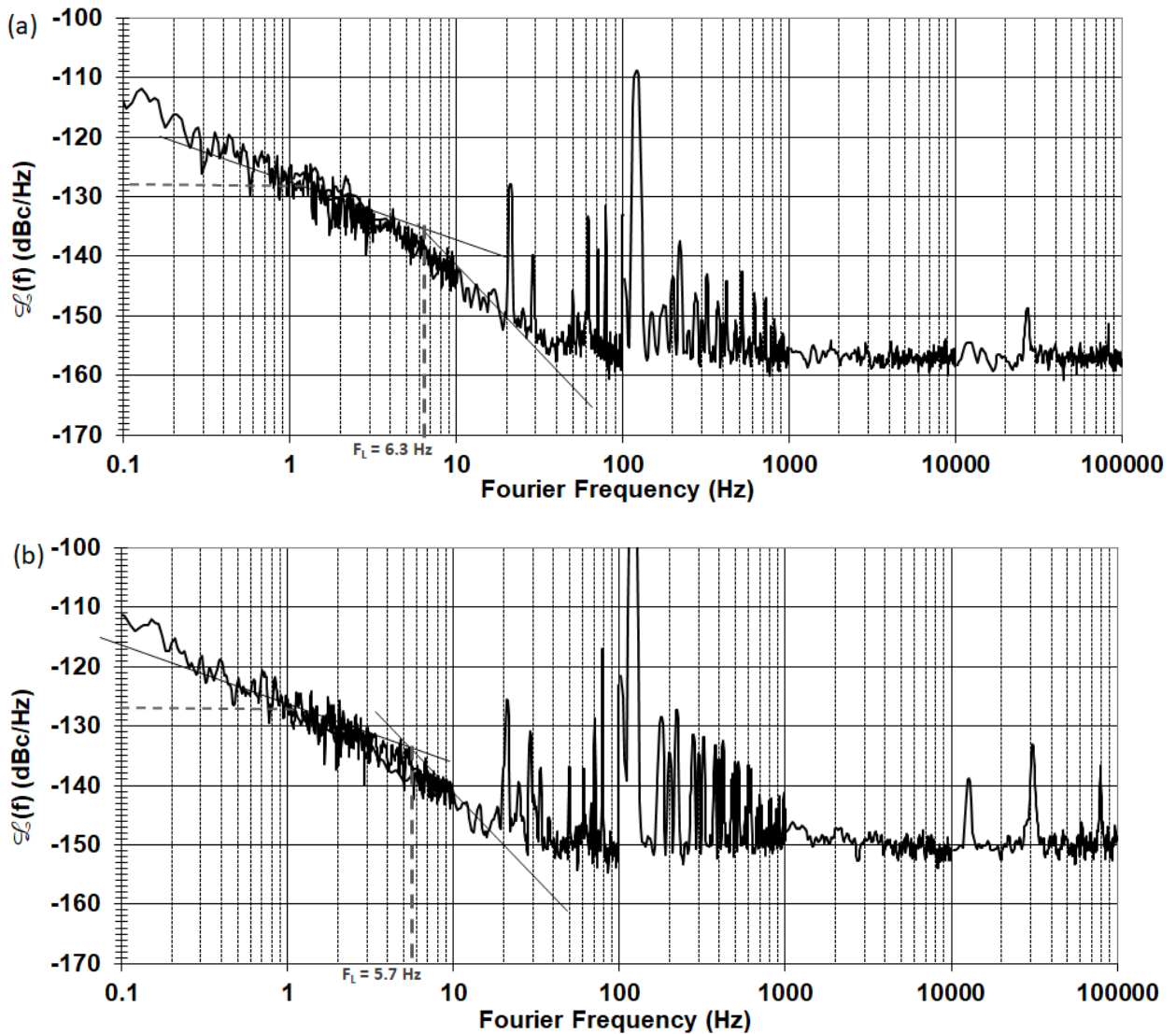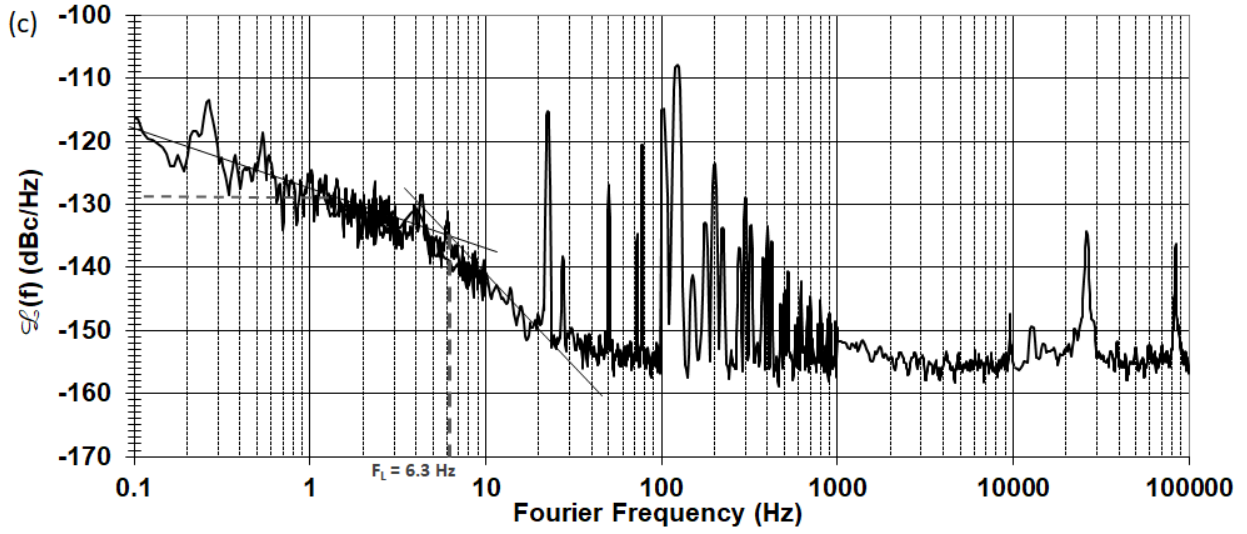
FIG. 12. Phase noise $\mathcal{L}$(f) of the resonator pairs according Fourier frequencies. (a) *LGT(1)-(2) pair*, (b) *LGT(1)-(3) pair*, (c) *LGT(2)-(3) pair*. Measured with T1-16 transformers with 200μW dissipated power.

The flicker floor of the short-term stability $\sigma_{y\_floor}$ is calculated for each pair and presented in Table IV. The optimization of the quality factor can be easily visualized by value of PSD and its asymptotic approach to determine the cut off frequency $F_L$ [8]. The flicker floor of the short-term stability is obtained from measurements of $\mathcal{L}$(1 Hz) and the cut off frequency $F_L$ (Figure 12). Considering precision of the measurement system, an error $\varepsilon$ in $\sigma_{y\_floor}$ is computed with $F_L$ à ±0.1 Hz and $\mathcal{L}$(1Hz) à ±2 dB.

TABLE IV. Short-term stability of the LGT resonators.

|  | $\sigma_{y\ floor} - \varepsilon$ | $\sigma_{y\ floor}$ | $\sigma_{y\ floor} + \varepsilon$ |
|---|---|---|---|
| *LGT(1)-(2)* | $2.34 \cdot 10^{-13}$ | $\mathbf{2.99 \cdot 10^{-13}}$ | $3.82 \cdot 10^{-13}$ |
| *LGT(1)-(3)* | $2.38 \cdot 10^{-13}$ | $\mathbf{3.04 \cdot 10^{-13}}$ | $3.90 \cdot 10^{-13}$ |
| *LGT(2)-(3)* | $2.08 \cdot 10^{-13}$ | $\mathbf{2.66 \cdot 10^{-13}}$ | $3.41 \cdot 10^{-13}$ |

Figure 13 presents the short-term stability $\sigma_{y\_floor}$ according the power dissipated by the resonators *LGT(1)-(2)*. The measured noise level is approximately constant for a dissipated power from 10 to almost 400 μW. This good stability should allow to apply more power to the resonator to have a better noise floor of the oscillator. This can result in having a good phase noise close to the carrier and a good flicker floor in the oscillator and these together should be easier than in quartz crystal oscillator.
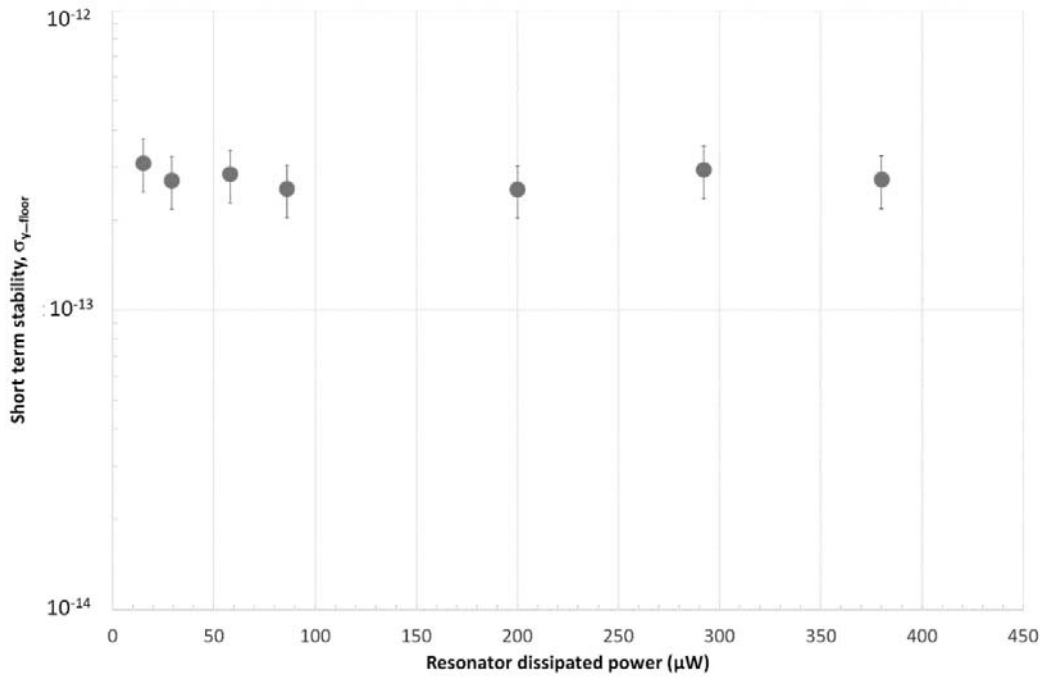
14

FIG. 13. Short-term stability $\sigma_{y\_floor}$ of the resonator $LGT_{(1)-(2)}$ pair according to the resonator dissipated power.

## IV. CONCLUSION

A passive measurement system based on carrier suppression using transformers to improve the loaded quality factor of the resonators has been implemented. Transformer matching is proposed to improve the loaded Q factor of the resonator and maximize the drive level power. Hence, this specific conditioning increases the phase noise of the resonators above the noise floor of measurement system. The noise floor of the measurement system is given according to the dissipated power showing that transformers do not degrade the noise floor of the measuring bench. Short-term stability of Langatate crystal resonators has been measured through impedance matching using transformers. It is evaluated according to the resonator driving power. The good stability should allow applying more power to the resonator to have a better noise floor of the oscillator. LGT drive sensitivity is lower than in SC-cut quartz more than a factor of ten, then, has a good phase noise close to the carrier and a good flicker floor in the oscillator and these together should be easier than in quartz crystal oscillator.

## ACKNOWLEDGMENTS

## DATA AVAILABILITY

The data that supports the findings of this study are available from the corresponding author upon reasonable request.

# REFERENCES

[1] K. H. Sann, (1968), "The measurement of near-carrier noise in microwave amplifiers," IEEE Trans. Microwave Theory Tech., MTT-16, 761. https://doi.org/10.1109/TMTT.1968.1126783.

[2] C. H. Horn, (1969), "A carrier suppression technique for measuring S/N and carrier/sideband ratios greater than 120 dB," in Proceeding of the 23rd Annual Frequency Control Symposium, Atlantic City, Electronic Industries Association Washington, D.C., pp. 6–8. https://doi.org/10.1109/FREQ.1969.199765.

[3] F. L. Walls, (1997), "Suppressed carrier based PM and AM noise measurement techniques," in Proceeding of the 51st Annual Frequency Control Symposium, Orlando, Institute of Electrical and Electronics Engineer Inc., Piscataway, NJ, pp. 485–492. https://doi.org/10.1109/FREQ.1997.638647.

[4] E. N. Ivanov, M. E. Tobar and R. A. Woode, (1997), "A study of noise phenomena in microwave components using an advanced noise measurement system," IEEE Trans. Ultrason. Ferroelect. Freq. Contr., 44, 161. https://doi.org/10.1109/58.585211.

[5] E. Rubiola, V. Giordano and J. Groslambert, (1999), "Very high frequency and microwave interferometric phase and amplitude noise measurements," Rev. Sci. Instrum., 70, 220. https://doi.org/10.1063/1.1149351.

[6] E. Rubiola, J. Groslambert, M. Brunet, and V. Giordano, (2000), "Flicker noise measurement of HF quartz resonators," IEEE Trans. Ultrason. Ferroelectr. Freq. Contr., 47, 361. https://doi.org/10.1109/58.827421.

[7] F. Sthal, M. Mourey, F. Marionnet, and W. F. Walls, (2000), "Phase noise measurements of 10 MHz BVA quartz crystal resonator," IEEE Trans. Ultrason. Ferroelectr. Freq. Contr., 47, 369. https://doi.org/10.1109/58.827422.

[8] F. Sthal, J. Imbaud, X. Vacheret, P. Salzenstein, G. Cibiel and S. Galliou, (2013), "Computation method for the short-term stability of quartz crystal resonators obtained from passive phase noise measures," IEEE Trans. Ultrason. Ferroelectr. Freq. Contr., 60, 1530. https://doi.org/10.1109/TUFFC.2013.2725.

[9] F. Sthal, M. Devel, J. Imbaud, R. Bourquin and G. Cibiel, (2015), "Fluctuation-dissipation theorem and 1/f noise of bulk acoustic wave cavities," Appl. Phys. Lett., 107, 103502. https://doi.org/10.1063/1.4930167.

[10]F. Sthal, M. Devel, J. Imbaud, R. Bourquin, S. Ghosh and G. Cibiel, (2016), "Study on the origin of 1/f noise in quartz resonators," J. Stat. Mech., 6, 054025. https://doi.org/10.1088/1742-5468/2016/05/054025.

[11]Y. Kim, (2003), "Amplitude-frequency effect of Y-cut Langanite and Langatate," IEEE Trans. on Ultrason., Ferroelect. and Freq. Contr., vol. 50, 1683, December. https://doi.org/10.1109/TUFFC.2003.1256309.

[12]J. Imbaud, S. Galliou, J.P. Romand, P. Abbé, and R. Bourquin, (2008), "Development of a 10 MHz oscillator working with an LGT crystal resonator: Preliminary results," IEEE Trans. Ultrason. Ferroelec. Freq. Contr., 55, 1913. https://doi.org/10.1109/TUFFC.883.

[13]J. Imbaud, G. Douchet and F. Sthal, (2010), "Passive noise analyses on langatate crystal resonators," in Proceeding of the IEEE Int. Freq. Cont. Symp., Newport beach, The Printing House, Inc., pp. 419-424. https://doi.org/10.1109/58.827422.

[14]J. Imbaud, J. J. Boy and F. Sthal, (2014), "LGT alternative quartz materials for ultra-stable oscillators," in Proceeding of the Proc.IEEE Int. Freq. Contr. Symp., Taipei, Tawain, IEEE Service Center, Piscataway, NJ, pp.32-39. https://doi.org/10.1109/FCS.2014.6859848.

[15]F. Sthal, S. Galliou, P. Abbé, X. Vacheret, and G. Cibiel, (2007), "Ultra-stable crystal ovens and simple characterization," Electron. Lett., 43, 900. https://doi.org/10.1049/el:20071052.

[16]N. Vorobyev, J. Imbaud, P. Abbé and F. Sthal, (2015), "Ultra-stable digitally controlled oven," Rev. Sci. Instrum., 86, 026102. https://doi.org/10.1063/1.4907542.

[17]IEC Standard, (1999), "Measurement of quartz crystal unit parameters by zero phase technique in a pi-network," IEC 60444-1:1986 + A1:1999, International Electrotechnical Commission, Paris.

[18]B. Boutahraoui, A. Nehari, J.J. Boy, X. Vacheret, M. Allani, H. Cabane, M. Dumortier, M. Derbal, K. Lebbou, "LGT (La$_3$Ga$_{5.5}$Ta$_{0.5}$O$_{14}$) langatate bulk crystal grown from the melt by Czochralski technique and characterization," Optical Materials, (2017), Vol. 65, March, pp. 103-105, https://doi.org/10.1016/j.optmat.2016.09.018.